Proceedings of the ASME 2024
International Design Engineering Technical Conferences and
Computers and Information in Engineering Conference
IDETC-CIE2024
August 25-28, 2024, Washington, DC

DETC2024-146367

REDUCING NONLINEAR VORTEX-INDUCED VIBRATIONS IN POWER LINES WITH MOVING NONLINEAR ABSORBERS

Ehab Basta
Department of Mechanical Engineering
Virginia Tech, Blacksburg, Virginia 24061

Sunit K. Gupta
Department of Mechanical Engineering
Virginia Tech, Blacksburg, Virginia 24061

Oumar R. Barry*
Department of Mechanical Engineering
Virginia Tech, Blacksburg, Virginia 24061

ABSTRACT

Aeolian vibration is a significant factor contributing to the fatigue failure of power transmission lines. The mitigation of such vibrations in power lines has traditionally been achieved using Stockbridge dampers along the line spans, which are modeled as fixed vibration absorbers. They largely depend on their resonant frequencies and placement on the cable. Therefore, given the stochastic nature of the wind, recent studies have explored the concept of dynamic/moving absorbers. Although the effectiveness of the moving absorber has been demonstrated in the literature to be superior to that of the fixed absorber, analyses have primarily been limited to linear cases and have not accounted for nonlinearity introduced by the moving absorber or the wind inflow on the powerline. Aiming to fill this gap, this work combines the nonlinearities from the fluctuating lift force modeled as a van der Pol oscillator, with a nonlinear moving absorber into a single model to investigate the effect of a nonlinear mobile damper relative to its linear counterpart. We observe that the system with a nonlinear moving absorber exhibits smaller amplitude oscillations when compared to its linear counterpart. This finding underscores the superior mitigation characteristics of nonlinear vibration absorbers and suggests the potential for designing an optimal nonlinear moving vibration absorber.

Keywords: Vortex-induced vibration · Moving absorber · Nonlinear absorber · Powerline · van der Pol Oscillator

1. INTRODUCTION

In the field of structural engineering, the intricate interaction between man-made infrastructure and external environmental forces introduces significant challenges. Among these, wind-induced and Aeolian vibrations present a persistent threat to the integrity of high-tension power transmission lines. Aeolian vibrations, characterized by small-amplitude, flexural oscillations in the crosswind direction, typically occur under light to moderate wind speeds [1]. Although these oscillations might seem to be minor amplitude, often less than the diameter of the conductor, their cumulative effect over time can lead to structural fatigue and the potential for catastrophic cable failure [2]. Consequently, understanding the dynamics of cable during Aeolian vibration is crucial for developing effective mitigation strategies.

The suppression of fatigue failure in power lines has traditionally been achieved through the use of Stockbridge dampers along the line spans [3-6]. However, studies indicate that the efficacy of Stockbridge dampers largely depends on their resonant frequencies and placement on the cable [7-9]. These dampers are usually positioned at the cable ends, where variable wind patterns may reduce their effectiveness. Specifically, fixed damper placements may coincide with nodal points within the frequency spectrum, significantly reducing their mitigation efficiency [8]. Thus, researchers have been investigating the use of dynamic/moving dampers for enhanced control. Notably, Bukhari et al. [4] introduced a concept of moving damper for power lines, while Kakou et al. [6] explored a PID-based control mechanism implemented on a mobile robot for both vibration suppression and line inspection. Their findings suggest that moving absorbers are more effective than fixed absorbers. However, these studies have yet to consider the impact of nonlinearity in the structure and the fluid-structure interaction, marking an essential direction for future research.

Due to the nonstationary and stochastic nature of wind, nonlinear dampers have been recognized as an optimal solution for vibration mitigation [10-14]. Their effectiveness is attributed to their ability to cover a broad frequency band for vibration attenuation [10,12] and their high level of robustness against unpredictable environmental conditions [13]. For instance, Samani and Pellicano [15] explored the dynamics of a beam under a moving load, comparing linear and nonlinear (specifically, cubic nonlinear) absorbers. They revealed that dampers with cubic nonlinear characteristics significantly reduced the maximum amplitude of vibrations. More recently, Zhang et al. [16] examined the performance of a nonlinear energy sink (NES) with cubic nonlinear damping. They found such an NES could outperform linear damping NES systems in reducing vibrations within nonlinear systems. It's critical to recognize that nonlinearity in these contexts can emerge from a variety of sources, including materials and environmental conditions, beyond just the absorbers themselves.

Aeolian vibrations are a type of resonance response most observed in slender, flexible structures, such as overhead power lines, when subjected to wind forces. These vibrations result from the shedding of vortices, known as the von Kármán vortex street, forming in the wake of the structure. The unsteady aerodynamic forces generated by this vortex shedding can resonate with structure, leading to Aeolian vibrations. Although Aeolian vibrations share characteristics with Vortex-Induced Vibrations (VIV) [17], they are distinct in their manifestation, typically occurring in air and involving higher frequencies and lower amplitude. For moving bodies, such as cylinders and sheets undergoing stretching, the simple sinusoidal force approximation used in basic fluid-structure interaction (FSI) models is often inadequate [18-20] due to the complex nature of the interaction involved. Consequently, more sophisticated models, like the coupled wake-oscillator models, have been developed to represent these phenomena more accurately. These models, which incorporate self-sustained oscillations through mechanisms such as negative damping, provide a closer approximation of the complex dynamics involved in VIV and Aeolian vibrations. Empirical validations of these models have demonstrated good agreement with experimental observations, establishing them as valuable tools for understanding and predicting the behavior of structures subjected to VIV [20,21].

In a review of existing literature, studies such as [4,6] have demonstrated the superior performance of moving absorbers over fixed absorbers in mitigating vibrations. However, these studies have not fully addressed the complexities introduced by nonlinearities, both from the absorber and wind forces. Given the critical role of nonlinear dynamics in the optimal design of vibration absorbers, especially under the conditions of high amplitude oscillations, this work introduces a novel approach. We examine a system in which a cable, modeled as an Euler-Bernoulli beam for its flexibility and bending characteristics, is integrated with a nonlinear moving absorber. The system is further coupled with a nonlinear lift force model, enhancing our understanding of its interactions with aerodynamic forces. The design of the moving damper system consists of a moving mass, a nonlinear spring, and a nonlinear damper, in addition to another mass, to effectively simulate the dynamic behavior of the absorber. The forces acting on the cable include pretension and the vortex-induced lift force, which are modeled using the van der Pol oscillator. This approach enables a more comprehensive exploration of the nonlinear cable's response to nonlinear aerodynamic excitations.

The rest of the paper is organized as follows. In Section 2, we briefly present the mathematical model for the beam-moving absorber system coupled with the van der Pol oscillator. The validation of the model and its difference from the sinusoidal force model will be shown in Section 3, followed by the effectiveness of the nonlinear moving absorber in vibration suppression, detailed in Section 4. Finally, some conclusions are drawn in Section 5.

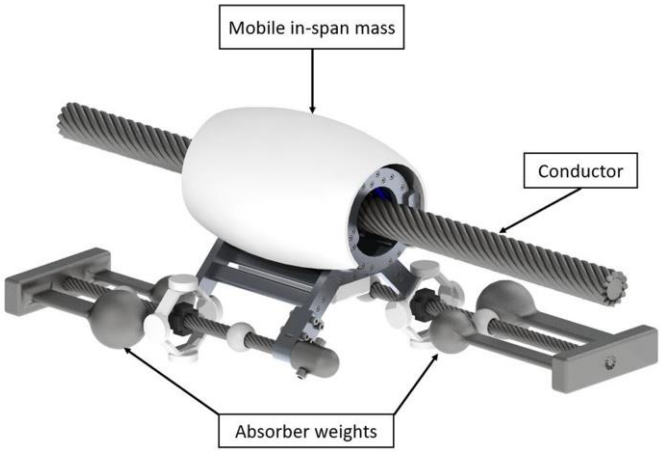

FIGURE 1: CONCEPTUAL DESIGN OF THE MOBILE DAMPER ATTACHED TO A POWER LINE CABLE [6]

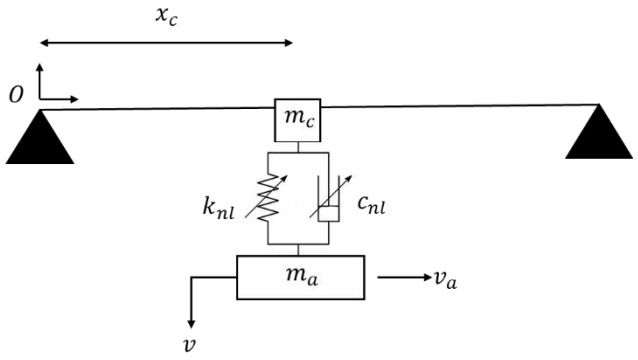

FIGURE 2: SCHEMATIC OF A SIMPLY SUPPORTED BEAM WITH A MOVING MASS-NONLINEAR SPRING-NONLINEAR DAMPER-MASS ABSORBER

2. MATHEMATICAL MODELING

The proposed conceptual design and the corresponding schematic of the moving vibration absorber are shown in Fig. 1

and 2, respectively. The system consists of a conductor with length L, a flexural rigidity of EI, and a mass per unit length m. Moreover, the Stockbridge damper consists of a clamped mass m_c and a suspended mass m_a. The damper has an equivalent linear/nonlinear stiffness (k, k_{nl}) and an equivalent linear/nonlinear damping coefficient (c, c_{nl}). Accordingly, the position vectors for the beam r_b, in span mass r_c, and the suspended mass r_a are given as

$$\begin{aligned} r_b &= x\boldsymbol{i} + y(x,t)\boldsymbol{j}, \\ r_c &= x_c(t)\boldsymbol{i} + y(x_c,t)\boldsymbol{j}, \\ r_a &= x_c(t)\boldsymbol{i} + v(t)\boldsymbol{j}, \end{aligned} \tag{1}$$

where x_c is the position of the absorber from the origin and v is the displacement of the absorber. Utilizing these position vectors, the total kinetic energy of the system is given by

$$\begin{aligned} K.E. = \frac{1}{2}m\int_0^L \{[\dot{y}(x,t)]^2\}dx \\ +\frac{1}{2}m_c[\dot{x}_c^2 + (\dot{y}(x_c,t) + y'(x_c,t)\cdot\dot{x}_c)^2] \\ +\frac{1}{2}m_a[\dot{x}_c^2 + \dot{v}^2] \end{aligned} \tag{2}$$

where the over dot denotes the derivative with respect to time t and the prime denotes the derivative with respect to the spatial coordinate x. The total potential energy can be defined as

$$\begin{aligned} \pi = \frac{1}{2}EI\int_0^L \{[y''(x,t)]^2\}dx + \frac{1}{2}k\,[y(x_c,t) - v]^2 \\ +\frac{1}{4}k_{nl}[y(x_c,t) - v]^4 \\ +\frac{1}{2}c[\dot{y}(x_c,t) + y'(x_c,t)\cdot\dot{x}_c - \dot{v}]^2 \\ +\frac{1}{4}c_{nl}[\dot{y}(x_c,t) + y'(x_c,t)\cdot\dot{x}_c - \dot{v}]^4 \end{aligned} \tag{3}$$

Finally, the work done by the axial force, i.e., the tension T on the system can be expressed as

$$W = \frac{1}{2}\int_0^L T\,y'^2 dx \tag{4}$$

Hence, the governing equations of motion for the system can be obtained by employing Hamilton's principle, which states

$$\delta\int_{t_1}^{t_2}(\pi - K.E. - W)dt = 0. \tag{5}$$

Substituting Eqs. (2), (3) and (4) in the above equation to get the following governing equations of motion as

$$EIy'''' + m\ddot{y} - Ty = F_L(x,t) - \{F_1 + F_2\}\,G(x,t) \tag{6}$$

$$m_a\,\ddot{v} = F_2 \tag{7}$$

where F_1 and F_2 are expressed as

$$\begin{aligned} F_1 = m_c\left(\frac{\partial^2 y}{\partial t^2} + 2\frac{\partial^2 y}{\partial x_r \partial t}\cdot\frac{dx_r}{dt} + \frac{\partial^2 y}{\partial x_r^2}\cdot\left(\frac{dx_r}{dt}\right)^2\right. \\ \left. +\frac{\partial y}{\partial x_r}\cdot\frac{d^2x_r}{dt^2}\right) \end{aligned} \tag{8a}$$

$$\begin{aligned} F_2 = [k[y - v] + b(y - v)^3 + c(\dot{y} + y'\dot{x}_c - \dot{v}) \\ + c(\dot{y} + y'\dot{x}_c - \dot{v})^3]|_{x=x_c} \end{aligned} \tag{8}$$

and $G(x,t)$ in Eq. (6) is used to define the location profile of the absorber using the Dirac delta functions and the Heaviside step function. The four location profiles correspond to

$$G = \begin{cases} g_1, & fixed\ absorber \\ g_2, & one-way\ moving\ absorber \\ g_3, & two-way\ moving\ absorber \\ g_4, & two-way\ two\ moving\ absorbers \end{cases}$$

where

$$g_1 = \delta(x - 0.02L), \tag{9a}$$

$$g_2 = \delta(x - V_a t)H(0.1L/V_a - t), \tag{9b}$$

$$\begin{aligned} g_3 = \delta(x - V_a t)H\left(\frac{0.1L}{V_a} - t\right) \\ +\delta\big(x - (0.2L - V_a t)\big)H(t \\ - 0.1L/V_a)H(0.2L/V_a - t), \end{aligned} \tag{9c}$$

$$\begin{aligned} g_4 = g_3 + \delta\big(x - (0.9L - V_a t)\big)H(0.1L/V_a - t) \\ +\delta(1.1L - V_a t)H(t \\ - 0.1L/V_a)H(0.2L/V_a - t). \end{aligned} \tag{9d}$$

Following Skop and Balasubramanian [23], the fluctuating fluid force, $F_L(x,t)$ can be defined in terms of fluctuating lift coefficient $C_L(x,t)$ as $F_L = \frac{\rho_f V_f^2 D C_L}{2}$, where C_L is governed by the following equation

$$C_L(x,t) = q(x,t) - \frac{2\alpha}{\omega_s}\dot{y}. \tag{10}$$

In the above equation, $q(x,t)$ represents the wake variable, and is further governed through a following nonlinear van der Pol oscillator

$$\ddot{q} - \omega_s G(C_{L0}^2 - 4q^2)\,\dot{q} + \omega_s^2 q = \omega_s F\dot{y}. \tag{11}$$

On combining the fluctuating force and van der Pol equations we get

$$F_L = \frac{\rho_f V_f^2 D}{2}\left(q(x,t) - \frac{2\alpha}{\omega_s}\dot{y}\right) \tag{12}$$

Thus, the combined governing equations of motion with a nonlinear absorber and a van der Pol oscillator after neglecting the Coriolis effect can be written as

$$EIy'''' + m\ddot{y} - Ty'' = \frac{\rho_f V_f^2 D}{2}\left(q - \frac{2\alpha}{\omega_s}\dot{y}\right) - \{F_1 + F_2\}\, G(x,t) \tag{13a}$$

$$m_a\, \ddot{v} = F_2 \tag{13b}$$

$$\ddot{q} - \omega_s G(C_{L0}^2 - 4q^2)\, \dot{q} + \omega_s^2 q = \omega_s F \dot{y} \tag{13c}$$

Using the eigenfunction expansion, we define $y(x,t)$ and $q(x,t)$ as

$$y(x,t) = \sum_{r=1}^{\infty} \phi_r(x) \cdot A_r(t) \quad \text{and} \quad q(x,t) = \sum_{r=1}^{\infty} \phi_r(x) \cdot \tilde{q}_r(t) \tag{14}$$

where $A_r(t), \tilde{q}_r(t)$ are unknown functions of time and $\phi_r(x)$ are the normalized eigenfunctions. Note that the eigenfunctions of the bare beam with tension [4] can be obtained as

$$\phi_r(x) = \sqrt{\frac{2}{ml}}\, sin\left[\left(\sqrt{\frac{-T}{2EI} + \sqrt{\frac{T^2}{4(EI)^2} + \frac{m\omega_r^2}{EI}}}\right) x\right] \tag{15}$$

where ω_r represents the natural frequencies of the bare beam and it is given by

$$\omega_r = \left(\frac{\pi}{L}\right)^2 \sqrt{\frac{EI}{m}\left(r^4 + \frac{r^2\, TL^2}{\pi^2 EI}\right)} \tag{16}$$

By substituting the assumed form of the solution into the governing equations (Eq. (13)) and performing Galerkin projection, we obtain following reduced order model as

$$\ddot{A_p} + 2\zeta\omega_p \dot{A_p} + \omega_p^2 A_p + \left[m_c\left(\sum_{i=1}^{\infty}\phi_i \ddot{A}_i\right) + k\left(\sum_{i=1}^{\infty}\{\phi_i A_i\} - v\right) + k_{nl}\left(\sum_{i=1}^{\infty}\{\phi_i A_i\} - v\right)\left(\sum_{j=1}^{\infty}\{\phi_j A_j\} - v\right)\left(\sum_{k=1}^{\infty}\{\phi_k A_k\} - v\right) + c\left(\sum_{i=1}^{\infty}\{\phi_i \dot{A}_\iota\} - \dot{v}\right) + c_{nl}\left(\sum_{i=1}^{\infty}\{\phi_i \dot{A}_\iota\} - \dot{v}\{\phi_i \dot{A}_i\}\right)\left(\sum_{j=1}^{\infty}\{\phi_j \dot{A}_j\} - \dot{v}\right)\left(\sum_{k=1}^{\infty}\{\phi_k \dot{A}_k\} - \dot{v}\right)\right]|_{x=x_c} \times \int_0^L \phi_p(x) G(x,t) = \frac{\rho_f V_f^2 D}{2m}\left(q_p - \frac{2\alpha}{\omega_s} A_p\right) \tag{17a}$$

$$m_a \ddot{v} = \left[k\left(\sum_{i=1}^{\infty}\{\phi_i A_i\} - v\right) + k_{nl}\left(\sum_{i=1}^{\infty}\{\phi_i A_i\} - v\right)\left(\sum_{j=1}^{\infty}\{\phi_j A_j\} - v\right)\left(\sum_{k=1}^{\infty}\{\phi_k A_k\} - v\right) + c\left(\sum_{k=1}^{\infty}\{\phi_i \dot{A}_\iota\} - \dot{v}\right) + c_{nl}\left(\sum_{i=1}^{\infty}\{\phi_i \dot{A}_i\} - \dot{v}\right)\left(\sum_{j=1}^{\infty}\{\phi_j \dot{A}_j\} - \dot{v}\right)\left(\sum_{k=1}^{\infty}\{\phi_k \dot{A}_k\} - \dot{v}\right)\right] \tag{17b}$$

$$\ddot{q}_p - \omega_S G C_{L0}^2\, \dot{q}_p - 4\omega_s G\left(\sum_{i=1}^{\infty}\dot{q}_p \cdot q_i^2 \int_0^L \phi_p^2 \cdot \phi_i^2\, dx + 2\sum_{i=1\ i\neq p}^{\infty} q_p q_i \dot{q}_i \int_0^L \phi_p^2 \cdot \phi_i^2\, dx\right) + \omega_s^2 q_p = \omega_s F \dot{A}_p \tag{17c}$$

We emphasize that the above set of ODEs include the dynamics for cable (A_p), moving nonlinear absorber (v) coupled with a van der Pol oscillator (q_p). In the subsequent sections, the simulations are obtained numerically by using ten mode expansion for more accurate results. Given the semi-empirical nature of the wake oscillator, it is crucial to validate the accuracy of the proposed model and demonstrate the differences between the wake oscillator model and a sinusoidal force model. This is shown in the next section.

3. Validation and Parameter Identification

In this section, we validate the accuracy of the proposed model. It should be noted that the van der Pol oscillator is derived from empirical observations and embodies theoretical principles, making it inherently a semi-empirical model. Thus, the damping and coupling parameters in the wake oscillator need to be identified. For this purpose, we compare the response of the system with the lift force modeled as a wake oscillator against the system with a sinusoidal lift force as presented in [4].

To achieve this, we establish the similarities between both models. Therefore, we substitute the stall term in Eq. (17a), α, as 0. This step ensures that the system's damping arises solely from structural damping and from the damping in the vibration absorber. Moreover, the excitation magnitude for sinusoidal forcing is amplified by the average of the steady-state response

of the wake variable q across the given frequency range. With these values of the excitation amplitude and stall parameter, the time history at a given frequency used in [4] and the frequency response curve for the first mode of the cable is analyzed and shown in Fig. 3.

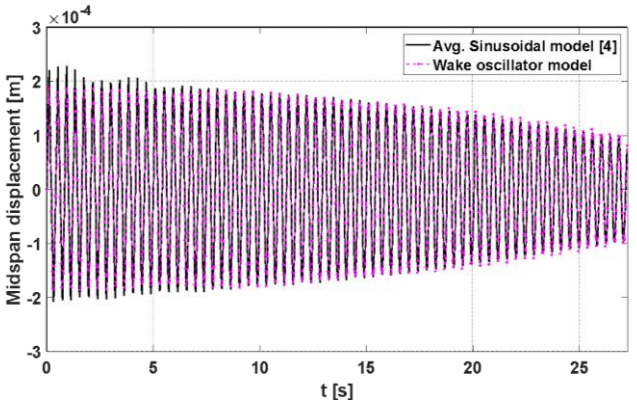

(a)

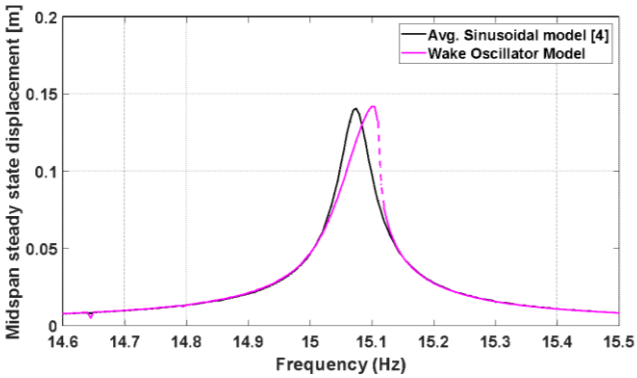

(b)

FIGURE 3: a) COMPARISONAND OF THE TIME RESPONSE OBTAINED BY TWO DIFFERENT FORCE MODELS AT $20Hz$ **b)** COMPARISON OF THE FREQUENCY RESPONSE OF THE CABLE WITH WAKE OSCILLATOR AND SINUSOIDAL FORCE CORRESPONDING AVERAGE VALUE

The comparison of time response of the system at the midspan with average sinusoidal forcing and wake forcing is shown in Fig. 3a. From Fig. 3a, we observe that for the given values of the primary system parameters in [4] and the values of the van der Pol oscillator i.e., $C_{l0} = 0.28, c_d = 1, F = 1.2534 \times 10^{-2}$ and $G = 0.3763$ [5], there is a good agreement between the sinusoidal lift-force model and the wake oscillator model. However, to elucidate the effect of the wake variable on the current system dynamics, we compare the corresponding frequency response curves for the first mode and is shown in Fig. 3b. The results show that the van der Pol model is approximately equivalent to the one corresponding to the sinusoidal oscillator; however, the later one could not capture the effect of nonlinearity in the system dynamics. This observation can be realized through the damping term in Eq. (17c), which is velocity-dependent and quadratic in nature. Nonlinearity is crucial in our system as it allows for a more accurate representation of the current nonlinear system.

Having established the differences and similarities between the current model and the sinusoidal forcing [4] to elucidate the effect of nonlinearity on the system, we present the effect of nonlinear absorbers in the wake-coupled system as compared to their linear counterpart as presented in [4] in the next section.

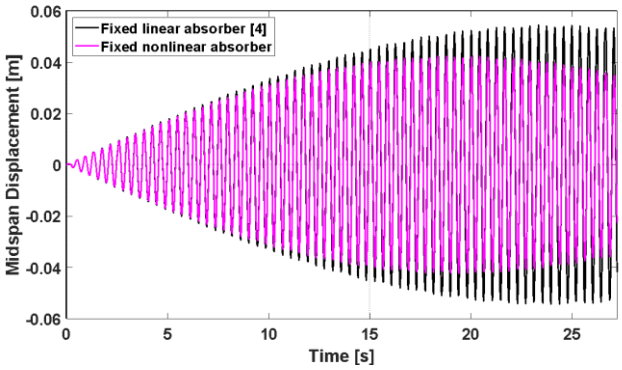

FIGURE 4: TIME RESPONSE AT THE MID-SPAN OF THE CONDUCTOR FOR A FIXED LINEAR ABSORBER AND A FIXED NONLINEAR ABSORBER AT $f = 2.415\ Hz$

4. Results and Discussion

In this section, we explore the effectiveness of the moving nonlinear absorber on vibration mitigation by investigating the effect of different location profiles on the system dynamics. Figures (4-7) depict the comparison of the time response of the system for the fixed absorber, the linear moving absorber, and the nonlinear moving absorber for different location profiles mentioned in Eq. (9). It should be noted that in all cases of different location profiles, the cable is excited at the primary resonance only. For the sake of comparison with the analysis presented in [4], we also place the fixed linear absorber at 2% of the conductor's length.

For the first case of location profile g_1, it can be observed from Fig. 4 that at *resonance*, the nonlinear absorber outperforms its linear counterpart at the same location and for the parameters listed in [4], i.e. $k_{nl} = 1356.96$ and $c_{nl} = 177\ N.s$. This can be attributed to the fact that at resonance, the amplitude of the system becomes maximum. causing the damping force from the nonlinear absorber to increase nonlinearly at resonance.

The comparison of the response of the cable with the fixed linear absorber, a moving linear absorber, and a moving nonlinear absorber is depicted in Fig. 5 for the second location profile, g_2. The moving absorber (linear and nonlinear) moves forward and stops after some time. As anticipated from [4], the moving absorber (green) shows an improvement over its fixed counterpart at resonance. The dynamic nature of the absorber

enables the absorber to sweep through more efficient locations along the length of the cable, which is unattainable by a fixed absorber. Furthermore, similar to the observation drawn from Fig. 4, a nonlinear moving absorber (purple curve in Fig. 5)

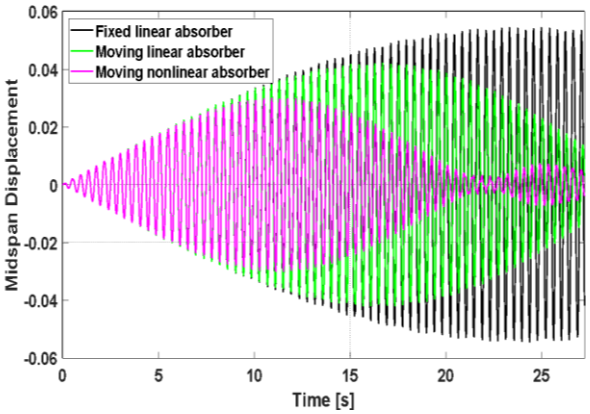

FIGURE 5: TIME RESPONSE AT THE MID-SPAN OF THE CONDUCTOR FOR A FIXED ABSORBER, A ONE WAY MOVING LINEAR ABSORBER AND A ONE WAY MOVING NONLINEAR ABSORBER AT $f = 2.415\ Hz$

further decreases the response of the cable as compared to a moving linear absorber.

The response of the forward-moving absorber can be significantly improved by implementing the third location profile g_3 (i.e., the absorber moves back and forth), as shown in Fig. 6. The vibration amplitude at resonance is reduced to less than half of that observed with a fixed linear absorber, over a period twice as long as the time taken by the absorber to move forward. Moreover, the moving nonlinear absorber fully envelopes the two-way moving linear absorber. Note that the response of the system in either case does not diminish to zero due to the limit cycle oscillations from the nonlinear van der Pol oscillator.

Finally, for a span length of $27.5m$, the results in Fig. 7 show a reduction of the vibration displacement when an additional nonlinear absorber is embedded at the other side of the cable corresponding to the location profile, g_4. The displacement of the moving linear absorber is still envelopes the moving nonlinear absorber most of the time, but due to the nonlinearities in the absorber, the response of the two-way moving absorbers on both sides of the cable exhibits some fluctuations before reaching the limit cycle.

The prior results show that at resonance and with an appropriate choice of parameters, a nonlinear moving absorber can significantly mitigate the vibration of the cable. With the availability of multiple parameters for the nonlinear moving absorber, such as the velocity, the nonlinear stiffness and damping as well as the effect of the van der Pol parameters, this becomes more of an optimization problem and is left for future work. The various parameters affecting the response of the system suggest that a parametric study and a performance assessment based on the efficiency of the absorber will enable us to further understand the potential improvement of the nonlinear moving absorber.

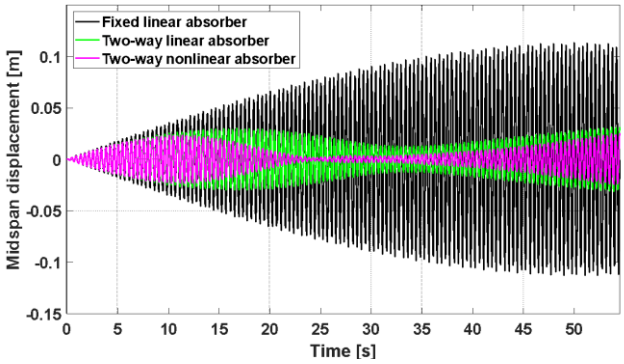

FIGURE 6: TIME RESPONSE AT THE MID-SPAN OF THE CONDUCTOR FOR A FIXED ABSORBER, A TWO WAY MOVING LINEAR ABSORBER AND A TWO WAY MOVING NONLINEAR ABSORBER AT $f = 2.415\ Hz$

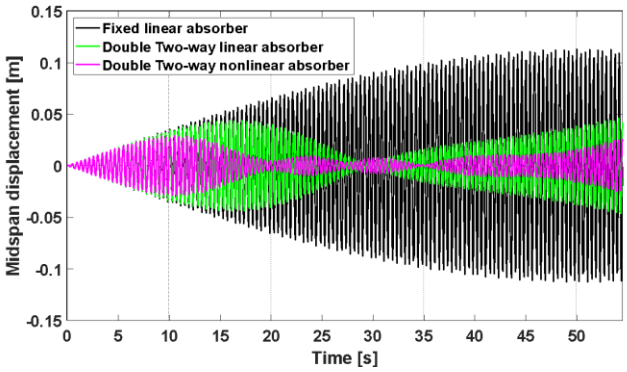

FIGURE 7: TIME RESPONSE AT THE MID-SPAN OF THE CONDUCTOR FOR A FIXED ABSORBER, TWO-WAY TWO MOVING LINEAR ABSORBERS AND TWO-WAY TWO MOVING NONLINEAR ABSORBERS AT $f = 2.415\ Hz$

5. CONCLUSIONS

In this study, we investigated the effectiveness of moving nonlinear vibration absorbers for different configurations on Aeolian vibration mitigation of nonlinear overhead powerlines. The nonlinear absorber comprised of a mass-nonlinear spring-nonlinear damper-mass subsystem and moves along a certain region to cover a wider range of frequencies. Moreover, the impact of the nonlinear moving absorber was elucidated by incorporating a nonlinear wake oscillator. The governing equations of motion were obtained through Hamilton's principle. The current model's parameters were identified by showing good agreement with the sinusoidal lift-force model. The time response at the first mode revealed that a fixed nonlinear absorber outperforms in mitigating the vibration amplitude of the conductor as compared to its linear counterpart at the same location. The mitigation was further enhanced by allowing the

nonlinear absorber to move forward for different configurations. We observed that a two-way moving nonlinear absorber was able to keep the amplitude at a very safe level at resonance. By adding an extra absorber on the other side, the response was significantly reduced. In all configurations, the linear moving absorber's response envelopes its nonlinear counterpart response and the nonlinear moving absorber showed better suppression of the amplitude at resonance.

ACKNOWLEDGEMENTS

This work was funded by (CAREER) - ECCS #1944032: Towards a Self-Powered Autonomous Robot for Intelligent Power Lines Vibration Control and Monitoring

REFERENCES

[1] *Transmission Line Reference Book: Wind-Induced Conductor Motion*. Palo Alto, Calif: EPRI, 1979.

[2] O. Barry, R. Long, and D. Oguamanam, "Simplified vibration model and analysis of a single-conductor transmission line with dampers," *Proceedings of the Institution of Mechanical Engineers, Part C: Journal of Mechanical Engineering Science*, vol. 231, no. 22, pp. 4150–4162, Jul. 2016.

[3] F. Foti and L. Martinelli, "Hysteretic behaviour of Stockbridge dampers: Modelling and parameter identification," *Mathematical Problems in Engineering*, vol. 2018, pp. 1–17, 2018.

[4] M. Bukhari, O. Barry, and E. Tanbour, "On the vibration analysis of power lines with moving dampers," *Journal of Vibration and Control*, vol. 24, no. 18, pp. 4096–4109, Jul. 2017.

[5] S. K. Gupta, A. L. Malla, and O. R. Barry, "Nonlinear vibration analysis of vortex-induced vibrations in overhead power lines with nonlinear vibration absorbers," *Nonlinear Dynamics*, vol. 103, no. 1, pp. 27–47, Jan. 2021.

[6] P. Kakou, M. Bukhari, J. Wang, and O. Barry, "On the vibration suppression of power lines using mobile damping robots," *Engineering Structures*, vol. 239, p. 112312, Jul. 2021.

[7] O. Barry, D. C. Oguamanam, and D. C. Lin, "Aeolian vibration of a single conductor with a Stockbridge damper," *Proceedings of the Institution of Mechanical Engineers, Part C: Journal of Mechanical Engineering Science*, vol. 227, no. 5, pp. 935–945, Jun. 2012.

[8] M. L. Lu and J. K. Chan, "An efficient algorithm for aeolian vibration of single conductor with multiple dampers," IEEE Transactions on Power Delivery, vol. 22, no. 3, pp. 1822–1829, Jul. 2007.

[9] O. Barry, J. W. Zu, and D. C. Oguamanam, "Nonlinear Dynamics of stockbridge dampers," Journal of Dynamic Systems, Measurement, and Control, vol. 137, no. 6, Jun. 2015. doi:10.1115/1.4029526

[10] A. Pazooki, A. Goodarzi, A. Khajepour, A. Soltani, and C. Porlier, "A novel approach for the design and analysis of nonlinear dampers for Automotive Suspensions," Journal of Vibration and Control, vol. 24, no. 14, pp. 3132–3147, Mar. 2017.

[11] E. Basta, M. Ghommem, and S. Emam, "Vibration suppression of nonlinear rotating metamaterial beams," Nonlinear Dynamics, vol. 101, no. 1, pp. 311–332, Jul. 2020.

[12] J. A. Main and N. P. Jones, "Free vibrations of taut cable with attached damper. II: Nonlinear damper," Journal of Engineering Mechanics, vol. 128, no. 10, pp. 1072–1081, Oct. 2002.

[13] H. Li, P. Zhang, G. Song, D. Patil, and Y. Mo, "Robustness study of the pounding tuned mass damper for vibration control of subsea jumpers," Smart Materials and Structures, vol. 24, no. 9, p. 095001, Jul. 2015.

[14] E. Basta, M. Ghommem, and S. Emam, "Flutter control and mitigation of limit cycle oscillations in aircraft wings using distributed vibration absorbers," Nonlinear Dynamics, vol. 106, no. 3, pp. 1975–2003, Oct. 2021.

[15] F. S. Samani and F. Pellicano, "Vibration reduction on beams subjected to moving loads using linear and nonlinear dynamic absorbers," Journal of Sound and Vibration, vol. 325, no. 4–5, pp. 742–754, Sep. 2009.

[16] Y. Zhang, X. Kong, C. Yue, and J. Guo, "Characteristic analysis and design of nonlinear energy sink with cubic damping considering frequency detuning," Nonlinear Dynamics, vol. 111, no. 17, pp. 15817–15836, Jul. 2023.

[17] R. D. Blevins, Flow-Induced Vibration. Malabar (Fl.): Krieger publ., 2001.

[18] S. Zuhra, N. Khan, M. Khan, S. Islam, W. Khan, and E. Bonyah, "Flow and heat transfer in water based liquid film fluids dispensed with graphene nanoparticles," Results in Physics, vol. 8, pp. 1143–1157, Mar. 2018.

[19] I. Khan and S. Shafie, “Rotating MHD flow of a generalized burgers’ fluid over an oscillating plate embedded in a porous medium,” Thermal Science, vol. 19, no. suppl. 1, pp. 183–190, 2015.

[20] N. S. Khan, S. Islam, T. Gul, I. Khan, W. Khan, and L. Ali, “Thin film flow of a second grade fluid in a porous medium past a stretching sheet with heat transfer,” Alexandria Engineering Journal, vol. 57, no. 2, pp. 1019–1031, Jun. 2018.

[21] W. D. Iwan and R. D. Blevins, “A model for vortex induced oscillation of structures,” Journal of Applied Mechanics, vol. 41, no. 3, pp. 581–586, Sep. 1974.

[22] R. A. Skop and O. M. Griffin, “On a theory for the vortex-excited oscillations of flexible cylindrical structures,” Journal of Sound and Vibration, vol. 41, no. 3, pp. 263–274, Aug. 1975.

[23] R. A. Skop and S. Balasubramanian, “A new twist on an old model for vortex-excited vibrations,” Journal of Fluids and Structures, vol. 11, no. 4, pp. 395–412, May 1997.